

# Scalar coupling limits with unitarity, stability and diphoton Higgs decay from LHC in an $U(1)'$ model plus a scalar dark matter

R. Martínez\*, J. Nisperuza†, F. Ochoa‡, J. P. Rubio§, C.F. Sierra¶  
 Departamento de Física, Universidad Nacional de Colombia,  
 Ciudad Universitaria, Bogotá D.C.

December 7, 2024

## Abstract

In the context of an nonuniversal  $U(1)'$  extension of the standard model free from anomalies, we introduce a complex scalar singlet candidate to be dark matter. In addition, an extra scalar doublet and a heavy scalar singlet are required to provide masses to all fermions and to break spontaneously the symmetries. From unitarity and stability of the Higgs potential, we find the full set of bounds and order relations for the scalar coupling constants. Using recent data from the CERN-LHC collider, we study the signal strenght of the diphoton Higgs decay  $R_{\gamma\gamma}$ , which imposes very stringent bounds to the scalar couplings and other scalar parameters. We obtain constraints in different scenarios of the space of parameters, where decays into dark matter may or may not contribute according to the mass of the scalar dark matter candidate.

## 1 Introduction

After the observation of an 125 GeV scalar particle at CERN-LHC by the ATLAS and CMS collaborations [1, 2], the electroweak symmetry breaking mechanism has been experimentally established. Now, one of the highest priorities of the LHC experiments is to measure precisely the strenghts of the couplings of the Higgs boson to fermions and vector bosons [3], which will allow to look for new states associated with the breaking symmetry mechanism in models beyond the standard model (SM) [4]. In particular, family non-universal  $U(1)'$  symmetry models have many well-established motivations. For example, they provide hints to solve the SM flavor puzzle [5], where regardless that all the fermions acquire masses at the same

---

\*e-mail: remartinezm@unal.edu.co

†e-mail: jlnisperu@unal.edu.co

‡e-mail: faochoap@unal.edu.co

§e-mail: jprubio@unal.edu.co

¶e-mail: cfsierraf@unal.edu.co

scale  $v = 246$  GeV, experimentally they exhibit very different mass values. These models also implies a new  $Z'$  neutral boson, which contains a large number of phenomenological consequences at low and high energies [6]. In addition of a new neutral gauge boson  $Z'$ , an extended fermion spectrum is necessary in order to obtain an anomaly-free theory. Also, the new symmetry requires an extended scalar sector in order to *i.*) generate the breaking of the new abelian symmetry and *ii.*) obtain heavy masses for the new  $Z'$  gauge boson and the extra fermion content.

On the other hand, the nonuniversal  $U(1)'$  extension of the the type introduced by authors in references [7] and [8], it was proposed an extended scalar sector with two scalar doublets and two singlets with nontrivial  $U(1)'$  charges (labeled for this particular model as  $U(1)_X$ ), where the lightest scalar singlet (denoted as  $\sigma_0$ ) is taken as candidate for dark matter (DM). Some phenomenological consequences of this model have been studied in the above references, with special emphasis in the neutral gauge and Yukawa sectors.

The main purpose of this paper is to determine some constraints on the parameters of the Higgs potential of the model, first by imposing theoretical bounds through unitarity and vacuum stability, and later by evaluating the new couplings of the observed Higgs boson with the extra scalar content using experimental data at CERN-LHC. In particular, the signal strenght of Higgs boson decays to diphotons offers a clean signal to constraint new physics associated to extra scalar sectors, where one loop contributions from the charged Higgs bosons is taken into account. Also, since the diphoton signal strenght depends on the branching ratio with the total Higgs boson decay, it is possible to evaluate the effects of a light DM component as an additional final state.

## 2 The Model

### 2.1 Particle content

The particle content of the model [7] is composed of ordinary SM particles and new exotic non-SM particles, as shown in Tables 1 and 2, respectively, where column  $G_{sm}$  indicates the transformation rules under the SM gauge group ( $SU(3)_c, SU(2)_L, U(1)_Y$ ), column  $U(1)_X$  contains the values of the new quantum number  $X$ , and in the column labeled *Feature*, we describe the type of field. Some properties of this spectrum are:

1. The  $U(1)_X$  symmetry is nonuniversal only in the left-handed SM quark sector: the quark family  $i = 3$  has  $X_3 = 1/3$  while families  $i = 1, 2$  have  $X_{1,2} = 0$ .
2. In order to ensure cancellation of the gauge chiral anomalies, the model includes in the quark sector three extra singlets  $T$  and  $J^n$ , where  $n = 1, 2$ . They are quasichiral, i.e. chiral under  $U(1)_X$  and vector-like under  $G_{sm}$ .
3. In addition, to obtain a realistic model compatible with oscillation data, we include new neutrinos  $(\nu_R^i)^c$  and  $N_R^i$  which may generate seesaw neutrino masses.
4. An additional scalar doublet  $\phi_2$  identical to  $\phi_1$  under  $G_{sm}$  but with different  $U(1)_X$  charges is included in order to avoid massless charged fermions, and where the indi-

vidual vacuum expectation values (VEVs) are related to the electroweak VEV through the relation  $v = \sqrt{v_1^2 + v_2^2}$ .

5. An extra scalar singlet  $\chi_0$  with VEV  $v_\chi$  is required to produce the symmetry breaking of the  $U(1)_X$  symmetry. We assume that it happens at a large scale  $v_\chi \gg v$ .
6. Another scalar singlet  $\sigma_0$  is introduced, which will be a DM candidate. Thus, this scalar must accomplish the following properties [8]:
  - (i) Since  $\sigma_0$  acquires nontrivial charge  $U(1)_X$ , it must be complex in order to obtain massive particles necessary for DM.
  - (ii) Terms involving odd powers of  $\sigma_0$  induce decay of the DM, which spoils the prediction of the model for the DM relic density. Thus, we demand the following global symmetry

$$\sigma_0 \rightarrow e^{i\theta} \sigma_0. \quad (1)$$

- (iii) In order to avoid the above symmetry to break spontaneously or new sources of decay,  $\sigma_0$  must not generate VEV during the evolution of the Universe. Thus, we demand  $v_\sigma = 0$ .

7. Finally, an extra neutral gauge boson  $Z'_\mu$  is required to obtain a local  $U(1)_X$  symmetry.

With the above conditions, we construct the Higgs potential.

## 2.2 Higgs potential

The most general, renormalizable,  $G_{sm} \times U(1)_X$  invariant potential and consistent with the global symmetry (1) is

$$\begin{aligned}
 V = & \mu_1^2 |\phi_1|^2 + \mu_2^2 |\phi_2|^2 + \mu_3^2 |\chi_0|^2 + \mu_4^2 |\sigma_0|^2 \\
 & + f_2 \left( \phi_2^\dagger \phi_1 \chi_0 + h.c. \right) \\
 & + \lambda_1 |\phi_1|^4 + \lambda_2 |\phi_2|^4 + \lambda_3 |\chi_0|^4 + \lambda_4 |\sigma_0|^4 \\
 & + |\phi_1|^2 [\lambda_6 |\chi_0|^2 + \lambda'_6 |\sigma_0|^2] \\
 & + |\phi_2|^2 [\lambda_7 |\chi_0|^2 + \lambda'_7 |\sigma_0|^2] \\
 & + \lambda_5 |\phi_1|^2 |\phi_2|^2 + \lambda'_5 \left| \phi_1^\dagger \phi_2 \right|^2 + \lambda_8 |\chi_0|^2 |\sigma_0|^2.
 \end{aligned} \quad (2)$$

As shown in [8], the above potential lead us to the following mass eigenvectors:

$$\begin{aligned}
 \begin{pmatrix} G^\pm \\ H^\pm \end{pmatrix} &= R_\beta \begin{pmatrix} \phi_1^\pm \\ \phi_2^\pm \end{pmatrix}, & \begin{pmatrix} G_0 \\ A_0 \end{pmatrix} &= R_\beta \begin{pmatrix} \zeta_1 \\ \zeta_2 \end{pmatrix}, \\
 \begin{pmatrix} h_0 \\ H_0 \end{pmatrix} &= R_\alpha \begin{pmatrix} \xi_1 \\ \xi_2 \end{pmatrix}, & \begin{pmatrix} H_\chi \\ G_\chi \end{pmatrix} &\sim I \begin{pmatrix} \xi_\chi \\ \zeta_\chi \end{pmatrix},
 \end{aligned} \quad (3)$$

where  $I$  is the identity, and the rotation matrices are defined according to

$$R_{\beta,\alpha} = \begin{pmatrix} C_{\beta,\alpha} & S_{\beta,\alpha} \\ -S_{\beta,\alpha} & C_{\beta,\alpha} \end{pmatrix}, \quad (4)$$

The rotation angles  $\beta$  and  $\alpha$  are:

$$\tan \beta = T_\beta = \frac{v_2}{v_1}, \quad (5)$$

$$\sin 2\alpha \approx \sin 2\beta \left[ 1 - \frac{\sqrt{2}C_{2\beta}S_{2\beta}v^2}{f_2v_\chi} \left( \hat{\lambda}_{11}C_\beta^2 - \hat{\lambda}_{12}C_{2\beta} - \hat{\lambda}_{22}S_\beta^2 \right) \right] \quad (6)$$

while the eigenvalues are:

$$\begin{aligned} M_{H^\pm}^2 &\approx M_{H_0}^2 \approx M_{A_0}^2 \approx -\frac{f_2v_\chi}{\sqrt{2}} \left( \frac{1 + T_\beta^2}{T_\beta} \right) \\ M_{H_\chi}^2 &\approx 2\hat{\lambda}_{33}v_\chi^2, \\ M_{h_0}^2 &\approx \frac{2v^2}{(1 + T_\beta^2)^2} \left( \hat{\lambda}_{11} + 2\hat{\lambda}_{12}T_\beta^2 + \hat{\lambda}_{22}T_\beta^4 \right). \end{aligned} \quad (7)$$

where we define the following parameters:

$$\begin{aligned} \hat{\lambda}_{11} &= \lambda_1, \quad \hat{\lambda}_{22} = \lambda_2, \quad \hat{\lambda}_{33} = \lambda_3 \\ \hat{\lambda}_{12} &= \frac{1}{2}(\lambda_5 + \lambda'_5), \end{aligned} \quad (8)$$

On the other hand, by assuming that the lightest scalar field  $h_0$  corresponds to the observed Higgs boson, we are interested in the following trilinear couplings:

$$V_{h_0} = g_{H^\pm} H^+ H^- h_0 + g_\sigma \sigma_0 \sigma_0^* h_0, \quad (9)$$

where the couplings are defined as

$$\begin{aligned} g_{H^\pm} &= vC_\beta (C_\beta^2 C_\alpha \lambda_5 + 2S_\beta^2 C_\alpha \lambda_1 - S_\beta C_\beta S_\alpha \lambda'_5) \\ &\quad + vS_\beta (S_\beta^2 S_\alpha \lambda_5 + 2C_\beta^2 S_\alpha \lambda_2 - S_\beta C_\beta C_\alpha \lambda'_5), \\ g_\sigma &= v(\lambda'_6 C_\alpha C_\beta + \lambda'_7 S_\alpha S_\beta). \end{aligned} \quad (10)$$

### 3 Theoretical constraints

We first consider the theoretical constraints of the Higgs potential from unitarity and vacuum stability.

#### 3.1 Unitarity

In order to calculate the tree unitarity bounds of the model, we use the LQT method [9] developed by Lee, Quigg and Thacker [10]. It is based in the unitarity condition of the  $S$ -matrix at tree level (through the optical theorem) and the change of the longitudinal components of the massive vector boson fields by the respective Goldstone bosons in the limit at high energies according to the equivalence theorem. This method has been used in the analysis of two Higgs doublet models (THDM) in previous works [11, 12] and recently in an extended THDM with an additional scalar singlet [13].

At high energies, the dominant contribution to the two-body scattering processes comes from the quartic terms of the potential. Thus, the unitarity bound for the  $s$ -wave amplitude of the  $\mathcal{M}$ -matrix in the partial wave decomposition

$$|a_0| \leq \frac{1}{2}, \quad (11)$$

is reduced to the condition

$$|Q| \leq 8\pi, \quad (12)$$

with  $Q$  all the quartic couplings in the scalar sector. In order to apply this condition, it is convenient to calculate the eigenvalues of the  $\mathcal{M}$ -quartic matrix  $Q$  in two particle processes. In our case, the quartic terms of the Higgs potential in Eq. (2) are:

$$\begin{aligned} V_4 = & \lambda_1 |\phi_1|^4 + \lambda_2 |\phi_2|^4 + \lambda_3 |\chi_0|^4 + \lambda_4 |\sigma_0|^4 \\ & + \lambda_5 |\phi_1|^2 |\phi_2|^2 + \lambda'_5 \left| \phi_1^\dagger \phi_2 \right|^2 + \lambda_8 |\chi_0|^2 |\sigma_0|^2 \\ & + |\phi_1|^2 [\lambda_6 |\chi_0|^2 + \lambda'_6 |\sigma_0|^2] \\ & + |\phi_2|^2 [\lambda_7 |\chi_0|^2 + \lambda'_7 |\sigma_0|^2], \end{aligned} \quad (13)$$

with the scalar field representations from tables 1 and 2. In this way according with the LQT method, the  $Q$ -matrix can be expressed as an  $18 \times 18$  matrix with three independent block diagonal matrices  $\mathcal{M}_1(6 \times 6)$ ,  $\mathcal{M}_2(9 \times 9)$  and  $\mathcal{M}_3(3 \times 3)$  which do not couple with each other due to charge conservation and CP-invariance [11]. First, In the basis  $(\omega_1^+ \omega_2^-, \omega_2^+ \omega_1^-, h_1 z_2, h_2 z_1, z_1 z_2, h_1 h_2)$  the symmetric submatrix  $\mathcal{M}_1$  is given by

$$\mathcal{M}_1 = \begin{pmatrix} 0 & \lambda_5 + \lambda'_5 & i\lambda'_5/2 & -i\lambda'_5/2 & \lambda'_5/2 & \lambda'_5/2 \\ * & 0 & -i\lambda'_5/2 & i\lambda'_5/2 & \lambda'_5/2 & \lambda'_5/2 \\ * & * & \lambda_5 + \lambda'_5 & 0 & 0 & 0 \\ * & * & * & \lambda_5 + \lambda'_5 & 0 & 0 \\ * & * & * & * & \lambda_5 + \lambda'_5 & 0 \\ * & * & * & * & * & \lambda_5 + \lambda'_5 \end{pmatrix} \quad (14)$$

with eigenvalues

$$\begin{aligned}
e_1 &= \lambda_5, \\
e_2 &= \lambda_5 + 2\lambda'_5, \\
f_{\pm} &= \pm\sqrt{\lambda_5(\lambda_5 + 2\lambda'_5)}, \\
f_1 &= f_2 = \lambda_5 + \lambda'_5.
\end{aligned} \tag{15}$$

The next basis of scattering processes corresponds to  $(\omega_1^+\omega_1^-, \omega_2^+\omega_2^-, \frac{z_1z_1}{\sqrt{2}}, \frac{z_2z_2}{\sqrt{2}}, \frac{h_1h_1}{\sqrt{2}}, \frac{h_2h_2}{\sqrt{2}}, \frac{z_3z_3}{\sqrt{2}}, \frac{h_3h_3}{\sqrt{2}}, \sigma_0^*\sigma_0)$  where the  $\sqrt{2}$  factor accounts for identical particles, where

$$\mathcal{M}_2 = \begin{pmatrix} 4\lambda_1 & \lambda_5 + \lambda'_5 & \sqrt{2}\lambda_1 & \frac{\lambda_5}{\sqrt{2}} & \sqrt{2}\lambda_1 & \frac{\lambda_5}{\sqrt{2}} & \frac{\lambda_6}{\sqrt{2}} & \frac{\lambda_6}{\sqrt{2}} & 2\lambda'_6 \\ * & 4\lambda_2 & \frac{\lambda_5}{\sqrt{2}} & \sqrt{2}\lambda_2 & \frac{\lambda_5}{\sqrt{2}} & \sqrt{2}\lambda_2 & \frac{\lambda_7}{\sqrt{2}} & \frac{\lambda_7}{\sqrt{2}} & 2\lambda'_7 \\ * & * & 3\lambda_1 & \frac{1}{2}(\lambda_5 + \lambda'_5) & \lambda_1 & \frac{1}{2}(\lambda_5 + \lambda'_5) & \frac{\lambda_6}{2} & \frac{\lambda_6}{2} & \sqrt{2}\lambda'_6 \\ * & * & * & 3\lambda_2 & \frac{1}{2}(\lambda_5 + \lambda'_5) & \lambda_2 & \frac{\lambda_7}{2} & \frac{\lambda_7}{2} & \sqrt{2}\lambda'_7 \\ * & * & * & * & 3\lambda_1 & \frac{1}{2}(\lambda_5 + \lambda'_5) & \frac{\lambda_6}{2} & \frac{\lambda_6}{2} & \sqrt{2}\lambda'_6 \\ * & * & * & * & * & 3\lambda_2 & \frac{\lambda_7}{2} & \frac{\lambda_7}{2} & \sqrt{2}\lambda'_7 \\ * & * & * & * & * & * & 3\lambda_3 & \lambda_3 & \sqrt{2}\lambda_8 \\ * & * & * & * & * & * & * & 3\lambda_3 & \sqrt{2}\lambda_8 \\ * & * & * & * & * & * & * & * & 24\lambda_4 \end{pmatrix} \tag{16}$$

Its analytical eigenvalues are  $2\lambda_1, 2\lambda_2, 2\lambda_3$  and

$$a_{\pm} = \lambda_1 + \lambda_2 \pm \sqrt{(\lambda_1 - \lambda_2)^2 + (\lambda'_5)^2}. \tag{17}$$

The remaining four eigenvalues  $b_j, j = 1, 2, 3, 4$  comes from the solutions of a quartic polynomial equation that is not included here, nevertheless it gives two double degenerate eigenvalues that according to (12) satisfy

$$\lambda_1 + \lambda_2 + \frac{2}{3}\lambda_3 + 4\lambda_4 \leq 16\pi. \tag{18}$$

Finally, in the basis  $(h_1z_1, h_2z_2, h_3z_3)$  we obtain:

$$\mathcal{M}_3 = \begin{pmatrix} 2\lambda_1 & 0 & 0 \\ 0 & 2\lambda_2 & 0 \\ 0 & 0 & 2\lambda_3 \end{pmatrix}. \tag{19}$$

Thus, taking the unitarity condition from Eq. (12), we find the bound

$$e_1, |e_2|, |f_{\pm}|, |f_1|, 2\lambda_1, 2\lambda_2, 2\lambda_3, |a_{\pm}|, |b_j| \leq 8\pi. \tag{20}$$

### 3.2 Vacuum stability

The stability condition in the strong sense of [14] can be implemented by the definition of the  $\underline{K}$  like matrices

$$\begin{aligned} \underline{K} &= \begin{pmatrix} \phi_1^\dagger \phi_1 & \phi_2^\dagger \phi_1 \\ \phi_1^\dagger \phi_2 & \phi_2^\dagger \phi_2 \end{pmatrix}, \quad \underline{L} = \begin{pmatrix} \chi_0^* \chi_0 & 0 \\ 0 & \sigma_0^* \sigma_0 \end{pmatrix}, \quad \underline{M} = \begin{pmatrix} \phi_1^\dagger \phi_1 & 0 \\ 0 & \chi_0^* \chi_0 \end{pmatrix} \\ \underline{N} &= \begin{pmatrix} \phi_1^\dagger \phi_1 & 0 \\ 0 & \sigma_0^* \sigma_0 \end{pmatrix}, \quad \underline{P} = \begin{pmatrix} \phi_2^\dagger \phi_2 & 0 \\ 0 & \chi_0^* \chi_0 \end{pmatrix}, \quad \underline{Q} = \begin{pmatrix} \phi_2^\dagger \phi_2 & 0 \\ 0 & \sigma_0^* \sigma_0 \end{pmatrix}. \end{aligned} \quad (21)$$

The above matrices can be decomposed in terms of the Pauli matrices. For example, the components of  $\underline{K}$  can be written as:

$$\underline{K}_{ij} = \frac{1}{2} (K_0 \delta_{ij} + K_a \sigma_{ij}^a), \quad (22)$$

where  $K_0 = \phi_i^\dagger \phi_i$  and  $K_a = (\phi_i^\dagger \phi_j) \sigma_{ij}^a$  for  $i, j \in \{1, 2\}$  and  $a = 1, 2, 3$ . Extending the above decomposition to all matrices, we obtain the following components:

$$\underline{K} : \begin{cases} \phi_1^\dagger \phi_1 = (K_0 + K_3)/2, & \phi_1^\dagger \phi_2 = (K_1 + iK_2)/2, \\ \phi_2^\dagger \phi_2 = (K_0 - K_3)/2, & \phi_2^\dagger \phi_1 = (K_1 - iK_2)/2, \end{cases} \quad (23)$$

$$\underline{L} : \begin{cases} \chi_0^* \chi_0 = (L_0 + L_3)/2, \\ \sigma_0^* \sigma_0 = (L_0 - L_3)/2, \end{cases} \quad (24)$$

$$\underline{M} : \begin{cases} \phi_1^\dagger \phi_1 = (M_0 + M_3)/2 \\ \chi_0^* \chi_0 = (M_0 - M_3)/2 \end{cases}, \quad \underline{N} : \begin{cases} \phi_1^\dagger \phi_1 = (N_0 + N_3)/2 \\ \sigma_0^* \sigma_0 = (N_0 - N_3)/2 \end{cases}, \quad (25)$$

$$\underline{P} : \begin{cases} \phi_2^\dagger \phi_2 = (P_0 + P_3)/2 \\ \chi_0^* \chi_0 = (P_0 - P_3)/2 \end{cases}, \quad \underline{Q} : \begin{cases} \phi_2^\dagger \phi_2 = (Q_0 + Q_3)/2 \\ \sigma_0^* \sigma_0 = (Q_0 - Q_3)/2. \end{cases} \quad (26)$$

Thus, the potential in Eq. (13) become:

$$V_4 = \sum_r V_{4r}, \quad r = K, L, M, N, P, Q, \quad (27)$$

which can be written as [14] :

$$V_{4r} = \eta_{r00} r_0^2 + 2r_0 \eta_r r_a + r_a E_r r_b, \quad (28)$$

with

$$\begin{aligned} \eta_{K00} &= \frac{1}{4}(\lambda_1 + \lambda_2 + \lambda_5), & \eta_{L00} &= \frac{1}{4}(\lambda_3 + \lambda_4 + \lambda_8), \\ \eta_{M00} &= \frac{1}{4}\lambda_6, & \eta_{N00} &= \frac{1}{4}\lambda'_6, & \eta_{P00} &= \frac{1}{4}\lambda_7, & \eta_{Q00} &= \frac{1}{4}\lambda'_7, \end{aligned} \quad (29)$$

$$\boldsymbol{\eta}_K = \frac{1}{4} \begin{pmatrix} 0 \\ 0 \\ \lambda_1 - \lambda_2 \end{pmatrix}, \quad \boldsymbol{\eta}_L = \frac{1}{4} \begin{pmatrix} 0 \\ 0 \\ \lambda_3 - \lambda_4 \end{pmatrix}, \quad (30)$$

$$\boldsymbol{\eta}_r = 0, \quad r = M, N, P, Q$$

$$E_K = \frac{1}{4} \begin{pmatrix} \lambda'_5 & 0 & 0 \\ 0 & \lambda'_5 & 0 \\ 0 & 0 & \lambda_1 + \lambda_2 - \lambda_5 \end{pmatrix}, \quad E_L = \frac{1}{4} \begin{pmatrix} 0 & 0 & 0 \\ 0 & 0 & 0 \\ 0 & 0 & \lambda_3 + \lambda_4 - \lambda_8 \end{pmatrix}. \quad (31)$$

The strong stability condition require that  $f_r(u_i) > 0$  for all  $u_i$  in a set  $I = \{u_1, \dots, u_n\}$  [14], where the function  $f_r(u)$  is defined as

$$f_r(u) = u + \eta_{r00} - \boldsymbol{\eta}_r^T (E_r - u)^{-1} \boldsymbol{\eta}_r, \quad (32)$$

and its derivative:

$$f'_r(u) = 1 - \boldsymbol{\eta}_r^T (E_r - u)^{-2} \boldsymbol{\eta}_r. \quad (33)$$

For example, if  $r = K$ , we obtain:

$$f_K(u) = u + \frac{1}{4}(\lambda_1 + \lambda_2 + \lambda_5) - \frac{(\lambda_1 - \lambda_2)^2}{4(\lambda_1 + \lambda_2 - \lambda_5 - 4u)},$$

$$f'_K(u) = 1 - \frac{(\lambda_1 - \lambda_2)^2}{(\lambda_1 + \lambda_2 - \lambda_5 - 4u)^2}.$$

The roots of the derivative are:

$$f'_K(u) = 0 \longrightarrow \begin{cases} u_1 = \frac{1}{4}(2\lambda_2 - \lambda_5), \\ u_2 = \frac{1}{4}(2\lambda_1 - \lambda_5). \end{cases}$$

We evaluate the stability condition  $f_K(u_i) > 0$  in the set  $I = \{0, u_1, u_2, \mu\}$ , where  $\mu = \lambda'_5/4$  corresponds to the doubly degenerated eigenvalue of the  $E_K$  matrix such that  $f_K(\mu)$  is finite and  $f'_K(\mu) \geq 0$ , obtaining:

$$f_K(0) > 0 \quad \rightarrow \quad 4\lambda_1\lambda_2 > \lambda_5^2. \quad (34)$$

$$f_K(u_{1,2}) > 0 \quad \rightarrow \quad \lambda_1 + \lambda_2 > 0, \quad (35)$$

$$f_K(\mu) > 0 \quad \rightarrow \quad 4\lambda_1\lambda_2 > (\lambda_5 + \lambda'_5)^2. \quad (36)$$

With an identical procedure for  $f_L(u_i) > 0$ , we obtain:

$$4\lambda_3\lambda_4 > \lambda_8^2, \quad (37)$$

$$\lambda_3 + \lambda_4 > 0, \quad (38)$$

The matrices  $E_r$  for  $r = M, N, P, Q$  are reduced trivially to one element (eigenvalue) due to (30)

$$\begin{aligned} V_{4M} &= M_a E_{Mab} M_b, \quad V_{4N} = N_a E_{Nab} N_b, \\ V_{4P} &= P_a E_{Pab} P_b, \quad V_{4Q} = Q_a E_{Qab} Q_b, \end{aligned} \quad (39)$$

obtaining from the condition  $f_r(0) > 0$

$$\lambda_6 > 0, \quad \lambda'_6 > 0, \quad \lambda_7 > 0, \quad \lambda'_7 > 0. \quad (40)$$

### 3.3 Combined constraints

The unitarity conditions (18) and (20) and the stability ones (34-38) and (40), can be combined in order to obtain a more suitable parameter space. In this way, the final combined conditions are

$$0 < \lambda_1 < 4\pi, \quad (41)$$

$$0 < \lambda_2 \leq 4\pi, \quad (42)$$

$$0 < \lambda_3 \leq 4\pi, \quad (43)$$

$$\lambda_4 > 0, \quad (44)$$

$$\lambda_5 \leq 8\pi, \quad (45)$$

$$\lambda_5 + 2\lambda'_5 \leq 8\pi \quad (46)$$

$$\lambda_1 + \lambda_2 + \frac{2}{3}\lambda_3 + 4\lambda_4 \leq 16\pi, \quad (47)$$

$$|\lambda_5| < 2\sqrt{\lambda_1\lambda_2}, \quad (48)$$

$$|\lambda_5 + \lambda'_5| < 2\sqrt{\lambda_1\lambda_2}, \quad (49)$$

$$|\lambda_8| < 2\sqrt{\lambda_3\lambda_4}, \quad (50)$$

$$\lambda_6 > 0, \quad \lambda'_6 > 0, \quad \lambda_7 > 0, \quad \lambda'_7 > 0. \quad (51)$$

## 4 Diphoton Higgs decay

In the SM, the decay of the Higgs boson to diphoton is mediated by fermions and charged vector bosons loops. In the  $U(1)'$  model, there is an additional contribution due to the charged Higgs boson loop, obtaining the total diphoton Higgs width [15]

$$\Gamma(h_0 \rightarrow \gamma\gamma) = \frac{\alpha^2 M_{h_0}^3}{256\pi^3 v^2} \left| F_1(\tau_W) + \sum_f N_{cf} Q_f^2 F_{1/2}(\tau_f) + g_{H^\pm} F_0(\tau_{H^\pm}) \right|^2, \quad (52)$$

where  $N_{cf}$  and  $Q_f$  are the color and electric charge factors, respectively, and:

$$\tau_a = \frac{4M_a^2}{M_{h_0}^2}, \quad (53)$$

for  $a = W, f$  and  $H^\pm$ . The loop factors are:

$$\begin{aligned} F_1 &= 2 + 3\tau + 3\tau(2 - \tau)f(\tau), \\ F_{1/2} &= -2\tau[1 + (1 - \tau)f(\tau)], \\ F_0 &= \tau[1 - \tau f(\tau)], \end{aligned} \quad (54)$$

with:

$$f(\tau) = \begin{cases} [\sin^{-1}(1/\sqrt{\tau})]^2, & \tau \geq 1 \\ -\frac{1}{4} [\ln(\eta_+/\eta_-) - i\pi]^2, & \tau < 1 \end{cases} \quad (55)$$

where  $\eta_\pm = 1 \pm \sqrt{1 - \tau}$ . Finally, the charged Higgs coupling  $g_{H^\pm}$  is given by the Eq. (10).

On the other hand, the theoretical signal strenght is defined as the ratio between the  $h_0 \rightarrow \gamma\gamma$  branching decay of the  $U(1)'$  model and the  $SM$  prediction:

$$R_{\gamma\gamma} = \frac{Br(h_0 \rightarrow \gamma\gamma)}{Br(h_0 \rightarrow \gamma\gamma)^{SM}}. \quad (56)$$

We identify two scenarios according to the mass of the DM candidate of the model:

- *Scenario I:* If  $M_\sigma > M_{h_0}/2 \approx 63$  GeV, the decay of the Higgs boson to DM pair is kinematically forbidden. By assuming that the final states of the Higgs boson decay are of SM nature, then the signal strenght can be approximated as

$$R_{\gamma\gamma} \approx \frac{\Gamma(h_0 \rightarrow \gamma\gamma)}{\Gamma(h_0 \rightarrow \gamma\gamma)^{SM}}. \quad (57)$$

where the width of the SM is the same as (52) without the  $F_0$  factor.

- *Scenario II:* If  $M_\sigma \leq M_{h_0}/2 \approx 63$  GeV, the decay of the Higgs boson to DM pair is allowed. In this case, the total decay width can be separated in decays to SM particles and decay to DM. Thus, we obtain:

$$R_{\gamma\gamma} \approx \frac{\Gamma(h_0 \rightarrow \gamma\gamma) \times \Gamma_{h_0}^{SM}}{\Gamma(h_0 \rightarrow \gamma\gamma)^{SM} \times [\Gamma_{h_0}^{SM} + \Gamma(h_0 \rightarrow \sigma\sigma)]}. \quad (58)$$

where  $\Gamma_{h_0}^{SM}$  is the total decay width of the SM Higgs boson, while the width to DM pair is:

$$\Gamma(h_0 \rightarrow \sigma\sigma^*) = \frac{g_\sigma^2}{2\pi M_{h_0}^2} \sqrt{1 - \frac{4M_{\sigma_0}^2}{M_{h_0}^2}}, \quad (59)$$

and the coupling  $g_\sigma$  is given in (10).

In order to evaluate some constraints from the diphoton decay, we reduce conveniently our space of parameters. First, since the scalar couplings  $\lambda_1$  and  $\lambda_2$  show the same theoretical constraints as observed in the subsection 3.3, we can assume only one characteristic diagonal coupling constant  $\lambda_D = \lambda_1 = \lambda_2$ . Thus, we suppose that each doublet  $\phi_1$  and  $\phi_2$  shows the same self-interaction separately. On the other hand, there are two types of mixing couplings between both doublets, distinguished by the coupling constants  $\lambda_5$  and  $\lambda'_5$ , as observed in the Higgs potential in Eq. (2). In this case, we can also assume only one coupling that characterize the mixing interaction between the scalar doublets. Thus, we choose  $\lambda_{12} = \lambda_5 = \lambda'_5$  as the mixing coupling between  $\phi_1$  and  $\phi_2$ . For the numerical analysis, it will be convenient to define the following ratio

$$r_\lambda = \frac{\lambda_{12}}{\lambda_D}. \quad (60)$$

With the above parametrization, the constraints from Eqs. (41), (42) and (49) become:

$$\begin{aligned} 0 < \lambda_D < 4\pi \\ |r_\lambda| < 1. \end{aligned} \quad (61)$$

For the interactions of the scalar doublets with the scalar singlet  $\sigma_0$ , we also assume the same coupling  $\lambda' = \lambda'_6 = \lambda'_7$ . Thus, the constraints in (51) become:

$$\lambda' > 0. \quad (62)$$

The charged and DM scalar coupling functions from Eqn. (10) with the above parametrization, become:

$$\begin{aligned} g_{H^\pm} &= v\lambda_D (S_{2\beta}S_{(\alpha+\beta)} + r_\lambda C_{2\beta}C_{(\alpha+\beta)}) \\ g_\sigma &= v\lambda' C_{\alpha-\beta}. \end{aligned} \quad (63)$$

Finally, the relation (6) between the rotation angles can be simplified by:

$$\sin 2\alpha \approx \sin 2\beta \left[ 1 + \frac{M_{h_0}^2}{M_{H^\pm}^2} \frac{C_{2\beta}^2(1-r_\lambda)}{1 - \frac{1}{2}S_{2\beta}(1-r_\lambda)} \right]. \quad (64)$$

We use the experimental data of the diphoton signal strength  $R_{\gamma\gamma} = 1.55_{-0.28}^{+0.33}$  obtained by ATLAS [16] and  $R_{\gamma\gamma} = 1.54_{-0.42}^{+0.46}$  at CMS [17] for  $M_{h_0} = 125.5$  GeV.

## 4.1 Scenario I

Taking into account the relation (64), the signal strength in (57) has the following free parameters:  $(T_\beta, \lambda_D, r_\lambda, M_{H^\pm})$ . The SM prediction for the diphoton branching is  $Br(h_0 \rightarrow \gamma\gamma)^{SM} = 2.28 \times 10^{-3}$ , while its total width is  $\Gamma_{h_0} = 4.07 \times 10^{-3}$  GeV for a 125 GeV SM Higgs boson [18]. Using these data, we obtain the following constraints:

1. Fig. 1 display contour plots in the plane  $T_\beta - \lambda_D$  for different values of the ratio  $r_\lambda$ . We fix the charged Higgs mass at  $M_{H^\pm} = 300$  GeV, while the dashed horizontal line at  $\lambda_D = 4\pi$  mark the upper theoretical limit according to (61). First, for  $r_\lambda < 0$ , the allowed regions exhibit maximum peaks at intermediate values of  $T_\beta$ , which exceed the theoretical limit when  $r_\lambda$  is near zero. For larger negative values of this ratio, the peak fall and the allowed band is drastically reduced to narrow intervals at small values of  $\lambda_D$ , as shown in the  $r_\lambda = -0.4$  plot. For  $r_\lambda \geq 0$ , the allowed  $\lambda_D$  intervals increase with  $T_\beta$ , as shown in the three lower plots. In this case, we also see that for larger values of  $r_\lambda$ , the allowed intervals shrink to a narrow region at small values of  $\lambda_D$ . In general, these figures show that small values of  $T_\beta$  and large values of  $r_\lambda$  are largely excluded. Thus, according to the definition (60), the scenary where  $\lambda_{12} \ll \lambda_D$  is favoured by the diphoton decay. We also find that the above regions is not sensitive to variations of the charged Higgs mass  $M_{H^\pm}$ .
2. In Fig 2, we show the allowed regions in the plane  $r_\lambda - \lambda_D$  for three values of  $T_\beta$  and with  $M_{H^\pm} = 300$  GeV. In this case we can obtain scenarios for the entire  $r_\lambda$  range from  $-1$  to  $1$ . For  $T_\beta = 0.5$  and  $1$  (small values), we see that  $\lambda_D$  is excluded in almost all the theoretical range for all the  $r_\lambda$  values. Only, narrow allowed intervals appears for very small  $\lambda_D$  coupling. In contrast, at  $T_\beta = 10$  (large values), the allowed values for  $\lambda_D$  increase in the vicinity of  $r_\lambda = 0$ .
3. Finally, Fig. 3 show contour regions in the plane  $(M_{H^\pm}, T_\beta)$  for three values of  $\lambda_D$ . In this case, and according to the previous plots, we fix the ratio at  $r_\lambda = 0$  which exhibits the largest allowed intervals. In general, we can appreciate that the allowed points is not very sensitive to variation of the mass of the charged Higgs boson. However, we see that the  $T_\beta$  allowed ranges increase for larger  $\lambda_D$  values. Thus, in the scenario without mixing coupling ( $r_\lambda = 0$ ), large scalar couplings  $\lambda_D$  shows broader allowed intervals at large  $T_\beta$  values.

## 4.2 Scenario II

In this case, the parameter space is extended to  $(T_\beta, \lambda_D, r_\lambda, M_{H^\pm}, \lambda', M_{\sigma_0})$ . First, we obtain in Fig. 4 the allowed points in the plane  $(M_{\sigma_0}, \lambda')$  for  $\lambda_D = 4, 6, 8$  and 12. The other parameters are fixed to be  $T_\beta = 10$ ,  $M_{H^\pm} = 300$  GeV and  $r_\lambda = 0$ . We can see that the coupling with the DM candidate takes small values at low mass. The limits on  $\lambda'$  increase for larger masses, near the kinematic limit at 63 GeV. We also see that large values of  $\lambda_D$  allow large couplings  $\lambda'$ .

On the other hand, in order to evaluate the effects of the  $\sigma_0$  coupling on the diphoton signal strength, we obtain again the contours in the plane  $(T_\beta, \lambda_D)$  for different coupling constants  $\lambda'$ . Fig. 5 show the allowed regions for  $\lambda' = 0.5, 1$  and 3, where we fix the values  $M_{\sigma_0} = 60$  GeV and  $r_\lambda = 0$ , which was previously obtained in Fig. 1. We see that the allowed points drops to very narrow intervals and small values of  $T_\beta$ .

Finally, we evaluate the ranges for  $\lambda'$  which does not exhibit an upper limit with only theoretical constraints. Fig. 6 shows plots in the plane  $(\lambda', T_\beta)$  for  $r_\lambda = 0$  and three values for  $\lambda_D$ . First, with  $\lambda_D = 1$ , we see that the  $\lambda'$  can be as large as 1.7 for  $T_\beta = 1$ . This upper limit increases quickly for larger couplings. For  $\lambda_D = 5$  and 10, the limits increase up to  $\lambda' = 9$  and 18, respectively.

## 5 Conclusions

Constraints on the scalar potential couplings of a nonuniversal  $U(1)'$  extension of the SM was obtained using unitarity and stability of the Higgs potential. Using recent data from CERN-LHC collider, we obtain allowed points of the scalar parameters compatible with the signal strength of diphoton Higgs decay. We conclude that

1. By combining the unitarity and stability conditions, we obtain individual bounds and order relations between coupling constants. In particular, the scalar interactions of the observed 125 GeV Higgs boson are controlled by the six parameters  $\lambda_{1,2,5}, \lambda'_{5,6,7}$ . The theoretical constraints impose positive bounds on  $\lambda_{1,2}$ , while order relations arise between  $\lambda_5, \lambda'_5$  and  $\lambda_{1,2}$ . On the other hand, the couplings associated with the scalar DM candidate  $\lambda'_{6,7}$  are only bounded from below.
2. The observed diphoton Higgs decay at LHC imposes phenomenological constraints on the above couplings as well as on other scalar parameters. Since the signal strength depends on the total decay of the Higgs boson there arises two possible scenarios. In the first one, decays into DM is forbidden for masses above  $M_{h_0}/2 \approx 63$  GeV. In this case, the couplings  $\lambda_{1,2} = \lambda_D$  obtain very stringent bounds, exhibiting narrow allowed intervals at small values controlled by  $T_\beta$  and its ratio with  $\lambda_{12}$ , where we assume  $\lambda_{12} = \lambda_5 = \lambda'_5$ . However, the allowed values exhibits very large enhancement for very special cases of  $T_\beta$  and  $r_\lambda$ . We also observe that the allowed regions is sensitive to the sign of  $\lambda_{12}$ . As for the absolute value of  $\lambda_{12}$ , we obtain that small ratios  $r_\lambda = \lambda_{12}/\lambda_D$  is favoured.

3. In the scenario where the mass of the DM candidate is below the kinematical threshold of 63 GeV, the signal strength become sensitive to the couplings  $\lambda'_{6,7} = \lambda'$  and  $M_{\sigma_0}$ . Although these couplings are not bounded from above by the theoretical constraints, we found allowed intervals consistent with LHC data on the diphoton decay. The limits increase the values of the coupling  $\lambda'$  for larger values of  $\lambda_D$ , and near  $T_\beta = 1$ .

## Acknowledgment

This work was supported by the Departamento Administrativo de Ciencia, Tecnología e Innovación (COLCIENCIAS) in Colombia

## References

- [1] G. Aad et al. [ATLAS Collaboration], Phys. Lett. B 716, 1 (2012) [arXiv:1207.7214 [hep-ex]].
- [2] S. Chatrchyan et al. [CMS Collaboration], Phys. Lett. B 716, 30 (2012) [arXiv:1207.7235 [hep-ex]].
- [3] M. Baak, J. Cuth, J. Haller, A. Hoecker, R. Kogler, K. Moenig, M. Schott and J. Stelzer, [arXiv:1407.3792v1 [hep-ph]]; J. Baglio, [arXiv:1408.6066v2 [hep-ph]]; G. Cacciapaglia, A. Deandrea, G. Drieu La Rochelle and J.P Flament, [arXiv:1210.8120v2 [hep-ph]].
- [4] S.L. Glashow, Nucl. Phys. 22, 579 (1961); S. Weinberg, Phys. Rev. Lett. 19, 1264 (1967); A. Salam, in *Elementary Particle Theory: Relativistic Groups and Analyticity (Nobel Symposium No. 8)*, edited by N.Svartholm (Almqvist and Wiksell, Stockholm, 1968), p. 367.
- [5] P. Langacker and M. Plumacher, Phys. Rev. D 62, 013006 (2000); K. Leroux and D. London, Phys. Lett. B 526, 97 (2002); S. Baek, J. H. Jeon, and C. S. Kim, Phys. Lett. B 641, 183 (2006).
- [6] For a review see A. Leike, Phys. Rep. 317, 143 (1999); J. Erler, P. Langacker, and T. J. Li, Phys. Rev. D 66, 015002 (2002); S. Hesselbach, F. Franke, and H. Fraas, Eur. Phys. J. C 23, 149 (2002).
- [7] R. Martinez, J. Nisperuza, F. Ochoa and J.P. Rubio, Phys. Rev. D 89, 056008 (2014).
- [8] R. Martinez, J. Nisperuza, F. Ochoa and J.P. Rubio, hep-ph:1408.5153.
- [9] Kladiva, Eur.Phys.J.**C46**: 81-91 (2006),
- [10] B. W. Lee, C. Quigg, and H. B. Thacker, Phys. Rev. **D16**, 1519 (1977).
- [11] A. Arhrib, *Unitarity constraints on scalar parameters of the standard and two Higgs doublets model*, hep-ph/0012353

- [12] A. G. Akeroyd, A. Arhrib, and E.M. Naimi, Phys.Lett. **B490** (2000) 119-124,
- [13] A. Drozd, B. Grzadkowski, J. F. Gunion, Yun Jiang, *Extending two-Higgs-doublet models by a singlet scalar field - the Case for Dark Matter*, hep-ph:1408.2106
- [14] M. Maniatis, A. von Manteuffel, O. Nachtmann, F. Nagel, Eur.Phys.J. **C48**, 805-823 (2006),
- [15] A. Djouadi, Phys. Rept. 459, 1 (2008).
- [16] G. Aad *et al.*, Phys. Lett B 726, 88 (2013).
- [17] S. Chatrchyan *et al.*, JHEP 06, 081 (2013).
- [18] K.A. Olive *et al.* (Particle Data Group), Chin. Phys. C, 38, 090001 (2014).

Table 1: Ordinary SM particle content, with  $i = 1, 2, 3$ 

<i>Spectrum</i>	$G_{sm}$	$U(1)_X$	<i>Feature</i>
$q_L^i = \begin{pmatrix} U^i \\ D^i \end{pmatrix}_L$	$(3, 2, 1/3)$	$1/3$ for $i = 3$ $0$ for $i = 1, 2$	chiral
$U_R^i$	$(3^*, 1, 4/3)$	$2/3$	chiral
$D_R^i$	$(3^*, 1, -2/3)$	$-1/3$	chiral
$\ell_L^i = \begin{pmatrix} \nu^i \\ e^i \end{pmatrix}_L$	$(1, 2, -1)$	$-1/3$	chiral
$e_R^i$	$(1, 1, -2)$	$-1$	chiral
$\phi_1 = \begin{pmatrix} \omega_1^+ \\ \frac{1}{\sqrt{2}}(v_1 + h_1 + iz_1) \end{pmatrix}$	$(1, 2, 1)$	$2/3$	Scalar Doublet
$W_\mu = \begin{pmatrix} W_\mu^3 & \sqrt{2}W_\mu^+ \\ \sqrt{2}W_\mu^- & -W_\mu^3 \end{pmatrix}$	$(1, 2 \times 2^*, 0)$	$0$	Vector
$B_\mu$	$(1, 1, 0)$	$0$	Vector

Table 2: Exotic non-SM particle content, with  $n = 1, 2$ 

<i>Spectrum</i>	$G_{sm}$	$U(1)_X$	<i>Feature</i>
$T_L$	$(3, 1, 4/3)$	$1/3$	quasi-chiral
$T_R$	$(3^*, 1, 4/3)$	$2/3$	quasi-chiral
$J_L^n$	$(3, 1, -2/3)$	$0$	quasi-chiral
$J_R^n$	$(3^*, 1, -2/3)$	$-1/3$	quasi-chiral
$(\nu_R^i)^c$	$(1, 1, 0)$	$-1/3$	Majorana
$N_R^i$	$(1, 1, 0)$	$0$	Majorana
$\phi_2 = \begin{pmatrix} \omega_2^+ \\ \frac{1}{\sqrt{2}}(v_2 + h_2 + iz_2) \end{pmatrix}$	$(1, 2, 1)$	$1/3$	Scalar doublet
$\chi_0 = \frac{1}{\sqrt{2}}(v_\chi + h_3 + iz_3)$	$(1, 1, 0)$	$-1/3$	Scalar singlet
$\sigma_0 = \frac{1}{\sqrt{2}}(v_\sigma + h_4 + iz_4)$	$(1, 1, 0)$	$-1/3$	Scalar singlet
$Z'_\mu$	$(1, 1, 0)$	$0$	Vector

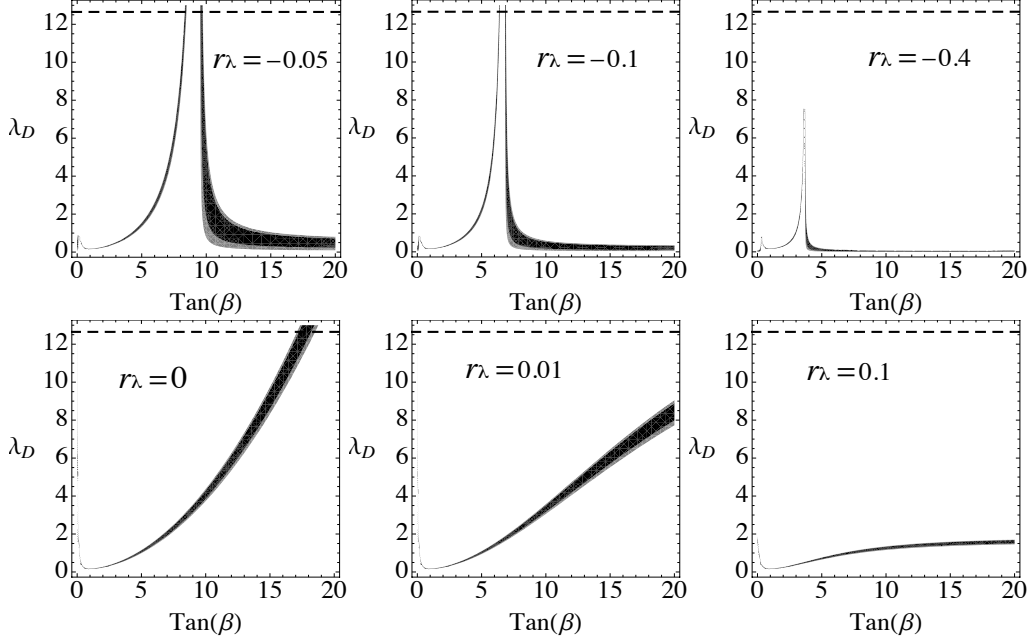


Figure 1: Allowed regions in the  $(T_\beta, \lambda_D)$  plane, compatible with the diphoton Higgs decay limits at ATLAS (black region) and CMS (gray region), for six values of the coupling ratio  $r_\lambda$ . The charged Higgs mass is fixed to be  $M_{H^\pm} = 300$  GeV. The dashed line fix the upper theoretical limit at  $\lambda_D = 4\pi$  from unitarity and stability of the Higgs potential.

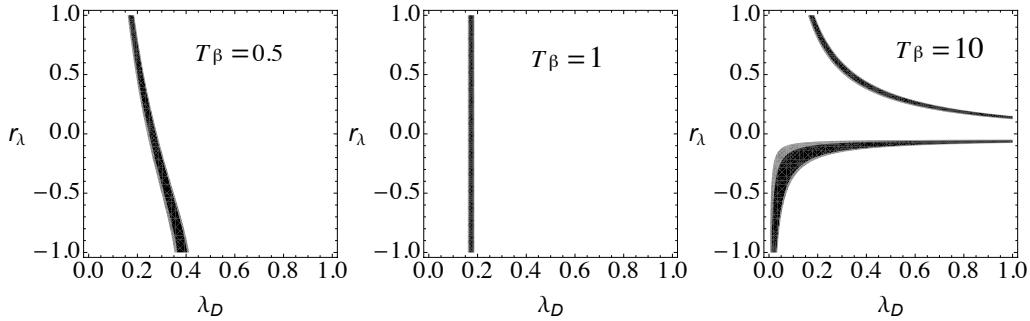


Figure 2: Allowed regions in the  $(\lambda_D, r_\lambda)$  plane, compatible with the diphoton Higgs decay limits at ATLAS (black region) and CMS (gray region), for three values of  $T_\beta$ . The charged Higgs mass is fixed to be  $M_{H^\pm} = 300$  GeV.

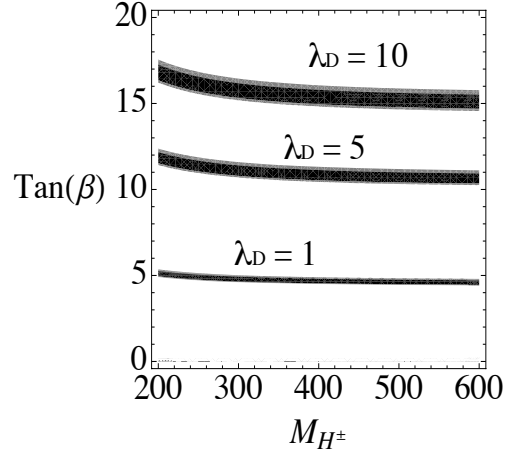


Figure 3: Allowed regions in the  $(M_{H^\pm}, T_\beta)$  plane, compatible with the diphoton Higgs decay limits at ATLAS (black region) and CMS (gray region), for three values of  $\lambda_D$ . The coupling ratio is fixed to be  $r_\lambda = 0$ .

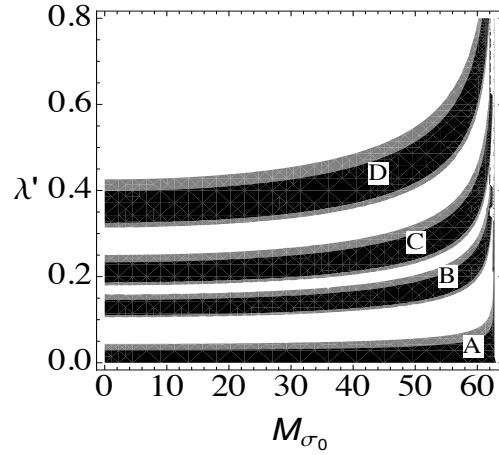


Figure 4: Allowed regions in the  $(M_{\sigma_0}, \lambda')$  plane, compatible with the diphoton Higgs decay limits at ATLAS (black region) and CMS (gray region), for  $\lambda_D = 4$ (A), 6(B), 8(C), and 12(D). The other parameters are fixed to be:  $T_\beta = 10$ ,  $M_{H^\pm} = 300$  GeV and  $r_\lambda = 0$ .

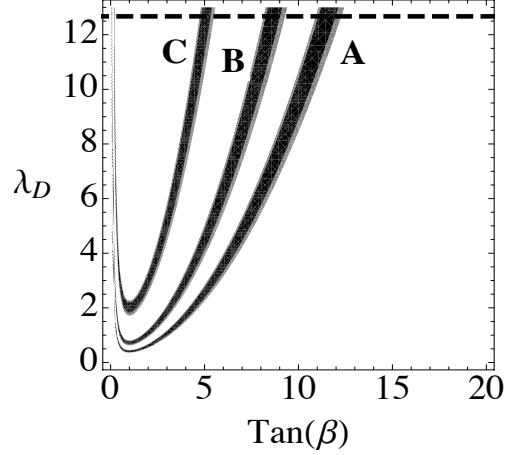


Figure 5: Allowed regions in the  $(\lambda_D, T_\beta)$  plane, compatible with the diphoton Higgs decay limits at ATLAS (black region) and CMS (gray region), for  $\lambda' = 0.5$ (A), 1(B), 3(C). The other parameters are fixed to be:  $M_{H^\pm} = 300$  GeV,  $M_{\sigma_0} = 60$  GeV and  $r_\lambda = 0$

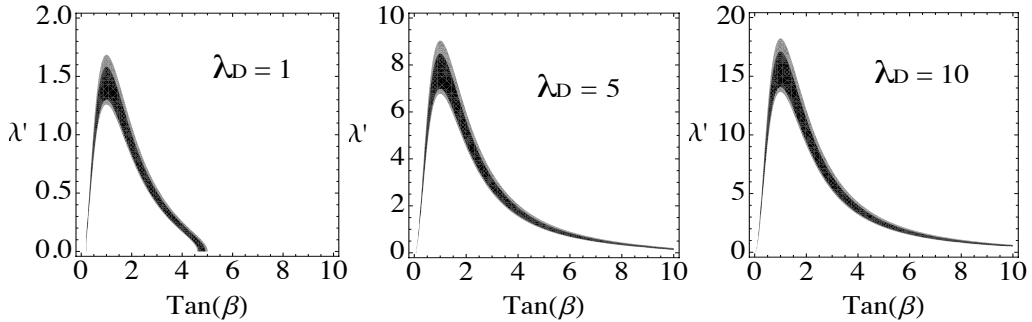


Figure 6: Allowed regions in the  $(T_\beta, \lambda')$  plane, compatible with the diphoton Higgs decay limits at ATLAS (black region) and CMS (gray region), for three values of  $\lambda_D$ . The other parameters are fixed to be:  $M_{H^\pm} = 300$  GeV,  $M_{\sigma_0} = 60$  GeV and  $r_\lambda = 0$ .